




Monolithic fabrication of vertical silicon nanowire gas sensor with a top porous copper electrode using glancing angle deposition

Naseem Abbas¹, Jun Kim¹, Jeongwoo Yeom¹, Seongmin Lee^{2,3}, Xun Lu^{1,4}, and Seok-min Kim^{1,2,3,*} 

¹Department of Mechanical Engineering, Chung-Ang University, 06974 Seoul, Republic of Korea

²Department of Mechanical System Engineering, Chung-Ang University, 06974 Seoul, Republic of Korea

³Department of Computer Science and Engineering, Chung-Ang University, 06974 Seoul, Republic of Korea

⁴Department of Mechanical Engineering, Yanbian University, 133002 Yanji, China

Received: 25 March 2020

Accepted: 4 January 2021

Published online:
27 January 2021

© The Author(s), under exclusive licence to Springer Science+Business Media, LLC part of Springer Nature 2021

ABSTRACT

Vertical Si nanowire (SiNW) gas sensor with a top porous electrode (TPE) has been reported as a highly sensitive, small footprint, and mass-producible gas sensor platform. In this article, a monolithic fabrication process for a vertical SiNW gas sensor using glancing angle deposition (GLAD) was proposed as a simple, low-cost, and large-area fabrication method, and the performance of the fabricated vertical SiNW gas sensor was evaluated via relative humidity measurement. The 1,000 nm length vertical SiNWs were uniformly fabricated on a 4-inch silicon wafer via GLAD at an oblique angle of 85° and a substrate rotation speed of 5 rpm. A Cu TPE was also fabricated via sequential GLAD without substrate rotation to realize the wafer-level vertical gas sensor from which multiple 2 × 2 cm² vertical SiNW gas sensors were obtained by dicing. To optimize the Cu TPE fabrication process, the effects of oblique angle and deposition thickness on the conductivity and porosity of the TPE were examined; subsequently, an oblique angle of 65° and a thickness of 100 nm were selected as the optimum conditions when considering humidity measurement sensitivity.

Abbreviations

NW Nanowire
TPE Top porous electrode
SiNW Si nanowire

GLAD Glancing angle deposition
E-beam Electron-beam
SEM Scanning electron microscopy

Address correspondence to E-mail: smkim@cau.ac.kr

<https://doi.org/10.1007/s10854-021-05255-4>

1 Introduction

Various configurations of semiconducting nanowire (NW) sensors have been developed as highly sensitive chemical and biological sensor platforms due to the high surface-to-volume ratio of the NW structures [1–6]. Most NW sensors have been designed as planar sensor platforms in which two electrodes are connected with semiconducting horizontal NWs [7–9] or semiconducting planar structures with vertical NWs [10–12]. In the planar NW sensor fabrication process, both the sensing and electrode areas are arranged on a substrate, thus there is a limitation on the number of sensors that can be fabricated on single substrate. To minimize the footprint of the sensor, a vertical NW sensor platform has been proposed in which the vertical NWs are formed on a bottom electrode and a top porous electrode (TPE) is formed on the vertical NWs [13–15]. The pores on the TPE provide a path for the gas analytes to pass through the NWs, and the TPE reliably connects to all the NWs. In et al. [13] fabricated vertical Si NWs (SiNWs) using a metal-assisted chemical etching process and a TPE using a lift-off process with a nanosphere lithographed sacrificial layer. Although they successfully demonstrated a vertical SiNW gas sensor, the fabrication process was relatively complex. To simplify the fabrication process, we previously reported a method to fabricate a TPE on metal-assisted chemically etched vertical SiNWs using glancing angle deposition (GLAD) [14]. GLAD is a physical vapor deposition process in which the substrate is tilted to obtain a large oblique angle (the angle between the surface normal and the deposition flux as shown in Fig. 1). At the initial stage of the deposition process, the evaporated nanoparticles are randomly attached to the flat substrate and the attached nanoparticles are grown as tilted NWs because the following evaporated nanoparticles are placed on top of the previous ones due to the self-shadowing effect [16, 17]. The selective deposition and growing of NWs are also possible when a pre-patterned substrate is used [18]. Although the diameter of the NWs fabricated via GLAD is mainly affected by the atomic mobility of the deposition material, the density and tilting angle of the NWs can be controlled by the oblique angle, and the length of the NWs can be controlled by the deposition time [19, 20]. In addition, the shape of the nanowires can be controlled by the rotation of the

substrate, thus one can obtain tilted NWs without substrate rotation and can obtain spiral or vertical NWs by controlling the substrate rotation speed [21]. Since the GLAD process is a wafer-scale fabrication process, and can provide both the vertical SiNWs and tilted Cu NWs in a single chamber by controlling substrate rotation and target material change, in this study, we proposed a wafer-scale monolithic fabrication method of the vertical SiNW gas sensor using a simple two-step GLAD process. A well-ordered array of isolated vertical SiNWs was produced via GLAD using substrate rotation at a high oblique angle, and the Cu TPE was sequentially fabricated via GLAD without substrate rotation on the vertical SiNWs. The Cu GLAD without substrate rotation was selected to generate a tilted Cu NWs on SiNWs because we thought the tilted Cu NWs has more opportunity to connect each other than the vertical Cu NWs to achieve high electrical conductivity. The effects of the GLAD conditions during the Cu TEP deposition on the conductivity and porosity of the TPE were examined and the optimum processing conditions were selected. Humidity measurement sensitivity was also studied to examine the performance of the proposed monolithic fabrication method for the vertical SiNW gas sensor.

2 Materials and methods

2.1 Monolithic fabrication method for vertical SiNW gas sensors via GLAD

Figure 1 shows schematics of the proposed monolithic fabrication process for the vertical SiNW sensor using the two-step GLAD. The upper part shows the schematics of experimental setup and conditions, and the bottom part shows the schematics of fabricated samples at the initial and final stages of each step. An electron-beam (E-beam) evaporator having a rotating 6-target-crucible changing system with a chamber diameter of 1 m (a modified SEE-7, Ultech Co., Ltd., Korea) was used in the experiment (Fig. 2a). For GLAD, a motorized substrate jig for controlling the oblique angle and substrate rotation speed was attached in the chamber, as shown in the upper parts of Fig. 1. In the 1st step GLAD process, the evaporation of Si material was carried out on a bare Si wafer with a relatively large oblique angle and

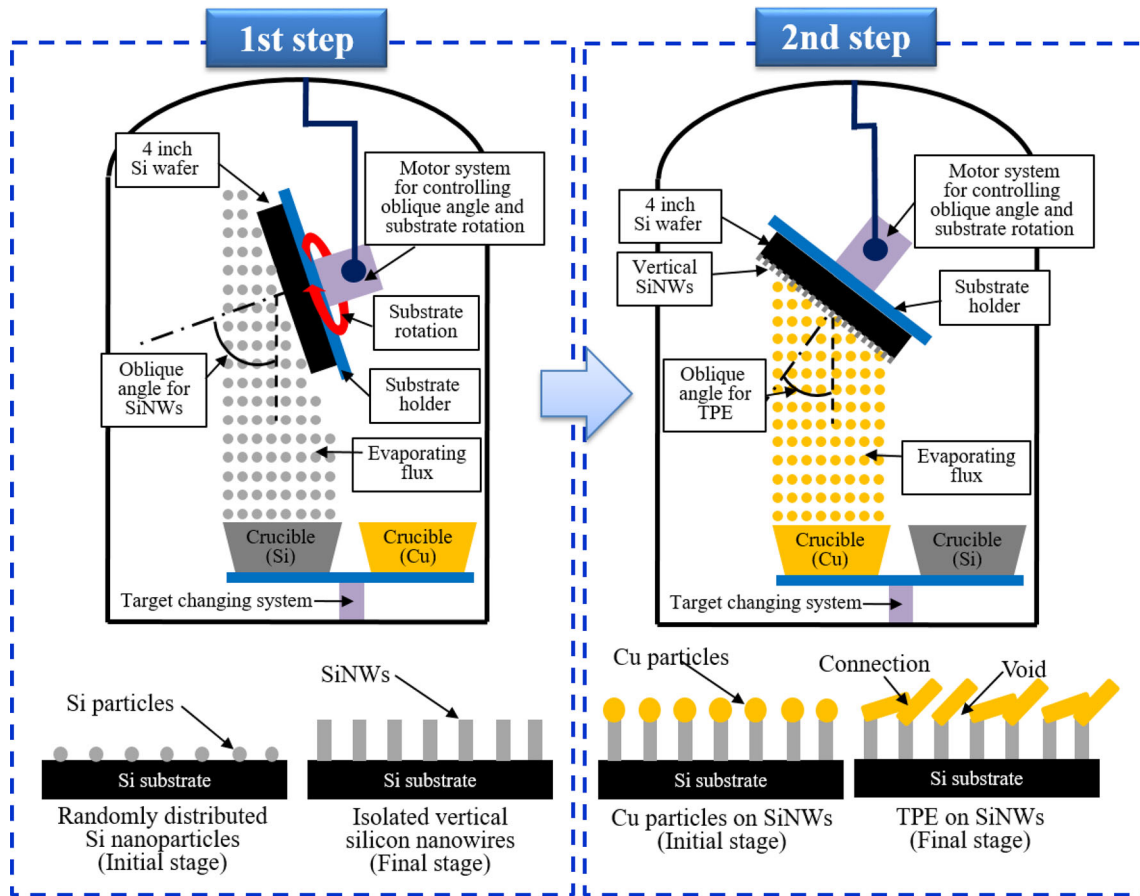


Fig. 1 Schematics of the monolithic fabrication process of vertical SiNWs and TPEs using GLAD. The upper parts show the system setup and conditions, and bottom parts show the fabricated samples at the initial and final stages of each step

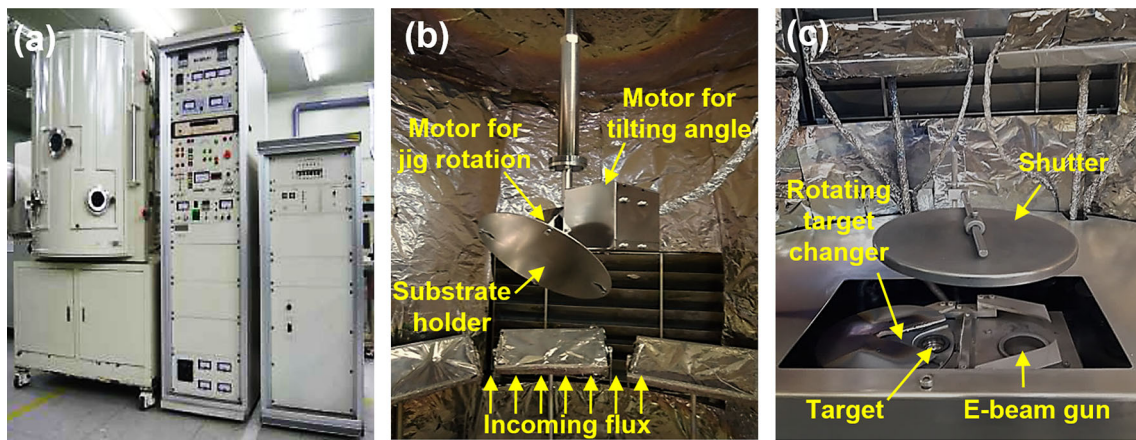


Fig. 2 Photographs of **a** the e-beam evaporator system, **b** the motorized substrate holder jig, and **c** the rotating target changing system used in the study

substrate rotation to generate isolated vertical SiNWs. At the initial stage of the 1st step GLAD process, the randomly distributed Si nanoparticles are arranged on the bare substrate and grow to the vertical SiNWs.

In the 2nd step GLAD process, the evaporating target material is changed to Cu and the evaporation was conducted on the vertical SiNWs with a relatively small oblique angle without substrate rotation. The

Cu nanoparticles are distributed on the top of SiNWs and grow to the tilted NWs. The oblique angle for 2nd Cu GLAD process was selected for that the tilted NWs partially contact together to realize the TPE as shown in Fig. 1. Figure 2 presents photographs of (a) the E-beam evaporator system, (b) the motorized substrate holder jig and (c) the rotating target changing system used in this study.

A boron (B)-doped p-type Si (100) 4-inch wafer with a resistivity of $\sim 5 \Omega \text{ cm}$ (Fine Science Co., Ltd., Korea) was used as the conductive bottom substrate for the vertical SiNW gas sensor. The substrate was sequentially cleaned with acetone, isopropyl alcohol, and deionized water and attached to the substrate jig in the chamber. Another B-doped p-type Si wafer was chopped and used as the target material for the vertical SiNWs, and the Cu pellets (99.999%, RND Korea, Co., Ltd., Korea) were used as the target material for the TPE. Each Si and Cu target materials were poured into the graphite crucibles and placed in the rotating target changing system of the E-beam evaporator (Fig. 2c). After the evacuation process with a pressure of $\sim 9.5 \times 10^{-7}$ Torr, the 1st GLAD process was carried out to fabricate vertical SiNWs on the Si substrate: the Si target was deposited on the substrate at a deposition rate of $\sim 5 \text{ \AA/s}$, an oblique angle of 85° , and a substrate rotating speed of 5 rpm. At the initial stage of the 1st GLAD process, the evaporated Si particles were randomly attached to the substrate and grew as vertical SiNWs due to the relatively fast substrate rotation [21]. The deposition time was controlled to obtain vertical SiNWs with a length of 1,000 nm. Figure 3 shows (a) top-view and (b) cross-sectional scanning electron microscopy (SEM) images of the fabricated vertical SiNWs. It clearly shows that the isolated vertical SiNWs were

uniformly fabricated on the substrate. The measured length of vertical SiNWs from the cross-sectional SEM image was $\sim 1000 \text{ nm}$ and the average diameter of SiNWs from the top-view SEM image was $\sim 90 \text{ nm}$. During the growing of the vertical SiNWs, the diameter slightly increased due to the atomic mobility of the material and some nanowires stopped growing because they entered the shadow area of the neighboring nanowires, which is in the nature of GLAD, as shown in Fig. 3b.

To fabricate the TPE, Cu was used as the evaporating target source and its sequential deposition on the vertical SiNWs was carried out at a deposition rate of $\sim 0.5 \text{ \AA/s}$, changing the oblique angle ($45\text{--}85^\circ$) without substrate rotation, and controlling the deposition time to obtain a Cu TPE layer with a thickness of 50–200 nm. In the 2nd step GLAD for Cu TPE, the substrate was not rotated to fabricate tilted Cu NW. At the initial stage of GLAD of the Cu material, the Cu nanoislands were formed on the top of each SiNWs and grew to create tilted NWs. Since the atomic mobility of Cu is relatively large, the diameter of the tilted Cu NW was larger than that of the SiNW and rapidly increased with increasing length. Therefore, the connection of neighboring Cu NWs could occur during GLAD without substrate rotation. Since the TPE of vertical SiNW sensor requires high conductivity and porosity for good electron transfer and gas permeability, respectively, and the probability of the connection between Cu NWs is affected by the tilting angle and length of Cu NWs, the effects of the oblique angle and deposition thickness of GLAD process on the resistance and porosity of the TPE were analyzed. After fabrication of the vertical SiNWs and a Cu TPE on a 4-inch Si substrate by the two-step GLAD process, the 4-inch

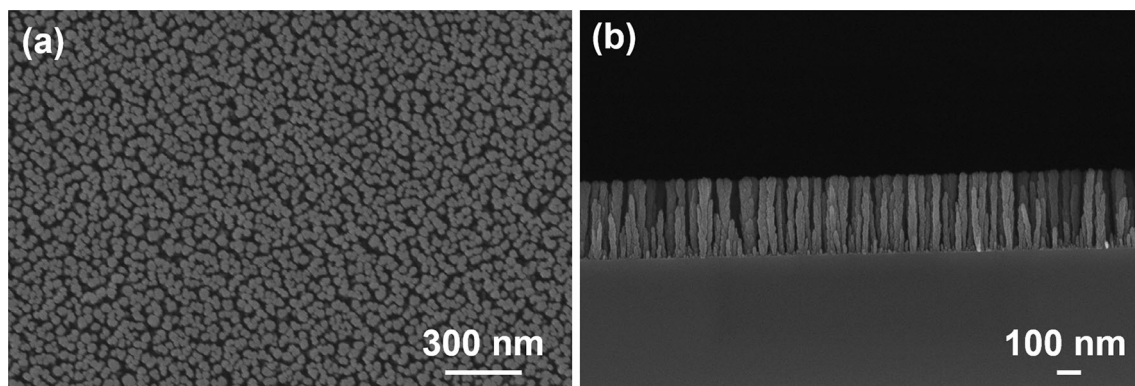


Fig. 3 **a** Top-view and **b** cross-sectional SEM images of fabricated vertical SiNWs with a height of 1000 nm

wafer-scale sensor was diced to 5×5 pieces and 21 vertical SiNW gas sensors with sizes of $\sim 2 \times 2 \text{ cm}^2$ were obtained (nine $2 \times 2 \text{ cm}^2$ sensors at the center of the wafer and twelve little smaller samples at the rim of the wafer).

2.2 Measurement of the conductivity and porosity of the TPE

To examine the conductivity of TPE, 4 electrical wires were attached at the 4 edges of the TPE on the diced vertical SiNW gas sensor using silver paste. The resistances between two electrical wires (6 combinations) were measured using a multimeter and the average value was calculated. The porosity of TPE was evaluated from the top-view SEM image of the fabricated TPE. The top-view SEM image was converted to a black-and-white image and the ratio of the void (black region) was calculated using the ImageJ program (National Institute of Health, USA).

2.3 Measurement of relative humidity using the fabricated vertical SiNW sensor

To evaluate the performance of the sensor, the relative humidity was measured using the fabricated vertical SiNW sensor in an acrylic humidity controllable chamber equipped with a humidity monitoring sensor and water vapor supply system. Since the resistance of the SiNWs decreased when water molecules were absorbed on their surfaces, the resistance between the bottom Si substrate and the Cu TPE were measured at various humidity levels (~ 25 to 85% relative humidity).

3 Results and analysis

3.1 Effects of the Cu TPE morphology on electrical conductivity and porosity

In this study, a series of investigations was carried out to assess the impact of various TPE morphologies used in the vertical SiNW sensor on humidity measurement sensitivity. For highly sensitive vertical SiNW gas sensor, high conductivity and porosity are essential for good electron transfer and gas permeability, respectively. Therefore, the GLAD process for the Cu TPE was optimized for maximizing the

conductivity and porosity of the TPE. Figure 4a–e shows top-view SEM images of the fabricated 100 nm-thick Cu TPE on vertical SiNWs via GLAD at various oblique angles of (a) 45° , (b) 55° , (c) 65° , (d) 75° , and (e) 85° . These clearly show that the connections of the tilted Cu NWs were decreased and the porosity was increased with increasing oblique angles. The cross-sectional SEM image in Fig. 4f clearly indicates that the Cu NWs were well connected with the Si NWs after GLAD at an oblique angle of 65° . To confirm the formation of top Cu NWs on bottom SiNWs, an -dispersive X-ray spectroscopy (EDX) analysis (FESEM-6330F (JEOL Ltd., Tokyo, Japan)) with an acceleration voltage of 18.0 kV was carried out and the measured spectra at the bottom NWs and top NWs are shown in Fig. 5. It clearly shows that Si is the dominant chemical at the bottom NWs and Cu is the dominant chemical at the top NWs. Some amount of Cu at the bottom NWs might be due to the diffusion of Cu molecules during the deposition process and EDX measurement. Some amount of Si at the top NWs might be due to the irregular heights of the SiNWs. The existence of oxygen was coming from the natural oxidization of Si materials.

For the quantitative analysis of the conductivity and porosity, the electrical resistance and porosity of TPEs on 5 diced gas sensors were examined. Figure 6 shows the measured electrical resistance and porosity of Cu TPE with a thickness of 100 nm. As the porosity of Cu TPE increased, the resistance also increased due to the lack of connections between the Cu NWs. Although high porosity values were observed for the Cu TPEs produced by GLAD at oblique angles of 75° and 85° , they did not show any conductivity. Since the resistance of the Si substrate for the fabricated $2 \times 2 \text{ cm}^2$ sensors was $\sim 21.5 \text{ k}\Omega$, the oblique angle of 65° was selected as the optimum condition for GLAD because the resistance value of $\sim 6 \Omega$ was acceptable for the vertical Si NWs gas sensor in this study, and higher porosity was observed than the TPEs fabricated at the oblique angles of 45° and 55° .

Since the connections between the neighboring Cu NWs are also affected by the length of tilted NWs, the effect of the Cu TPE layer thickness on the electrical resistance and porosity was analyzed. The vertical SiNW gas sensors with a TPE deposited at an oblique angle of 65° with various thicknesses (50–200 nm) were fabricated, as shown in Fig. 7, and the electrical resistance and porosity of TPE with different

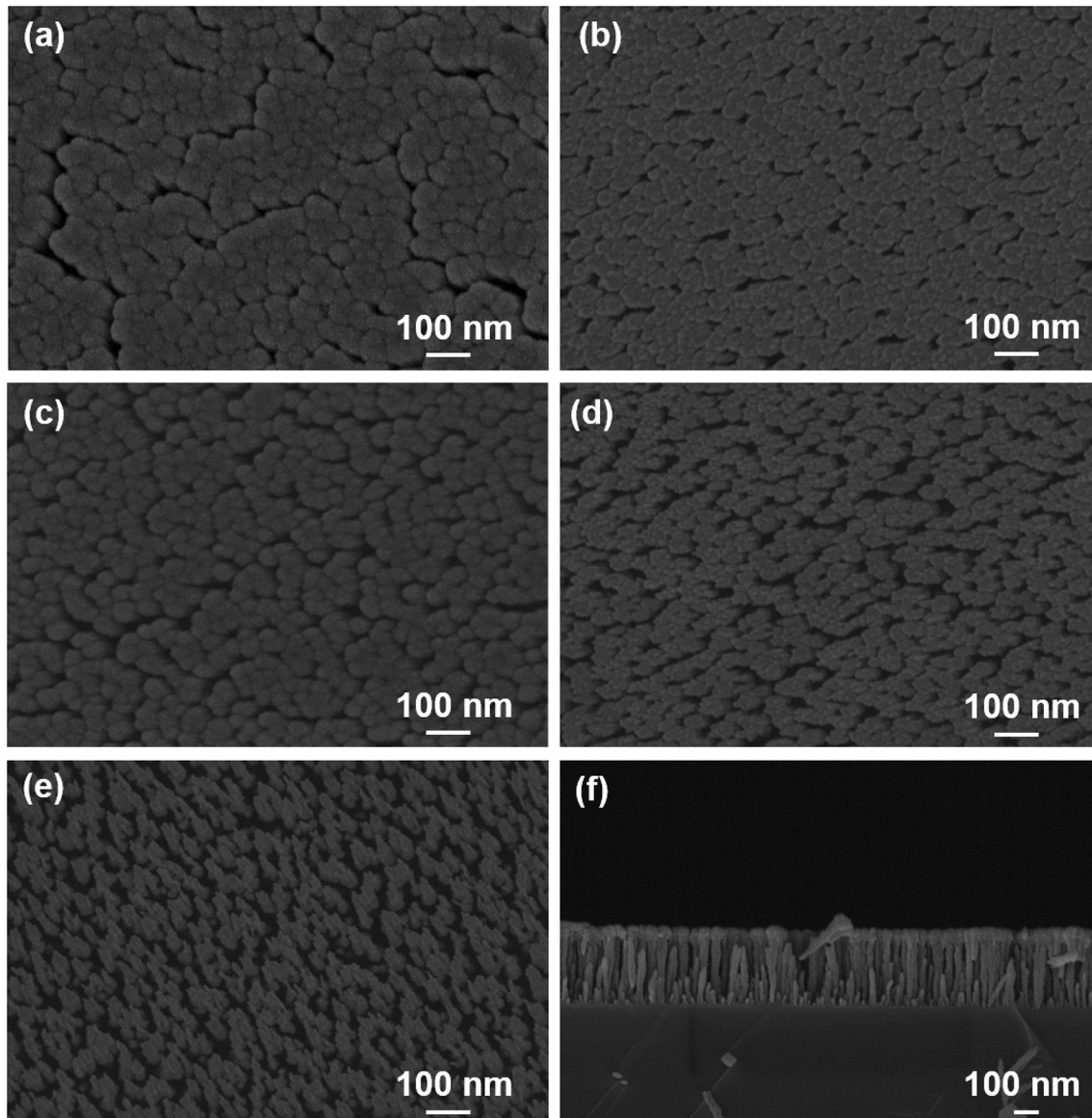


Fig. 4 Top-view SEM images of a fabricated 100 nm-thick Cu NW TPE on vertical Si NWs via GLAD at oblique angles of **a** 45°, **b** 55°, **c** 65°, **d** 75°, and **e** 85° and **f** a cross-sectional SEM image

thickness were measured, as shown in Fig. 8. As expected, the connections between neighboring Cu NWs increased with increasing thickness and the electrical resistance and porosity decreased. The maximum porosity was observed at a TPE thickness of 50 nm, but there was no electrical conductivity due to the lack of Cu NW connections.

of the vertical Si NWs with the Cu NW TPE fabricated by GLAD at an oblique angle of 65°

3.2 Effects of Cu TPE morphology on humidity measurement sensitivity

Although the electrical conductivity and porosity of the Cu TPE were analyzed, the optimum fabrication conditions for the Cu TPE should be selected to maximize the sensitivity of the SiNW gas sensor. Hence, relative humidity measurements were carried out in the humidity range of 25–85% to examine the performance of fabricated SiNW gas sensor. Since the initial resistances between the bottom electrode (Si substrate) and Cu TPE were not exactly same

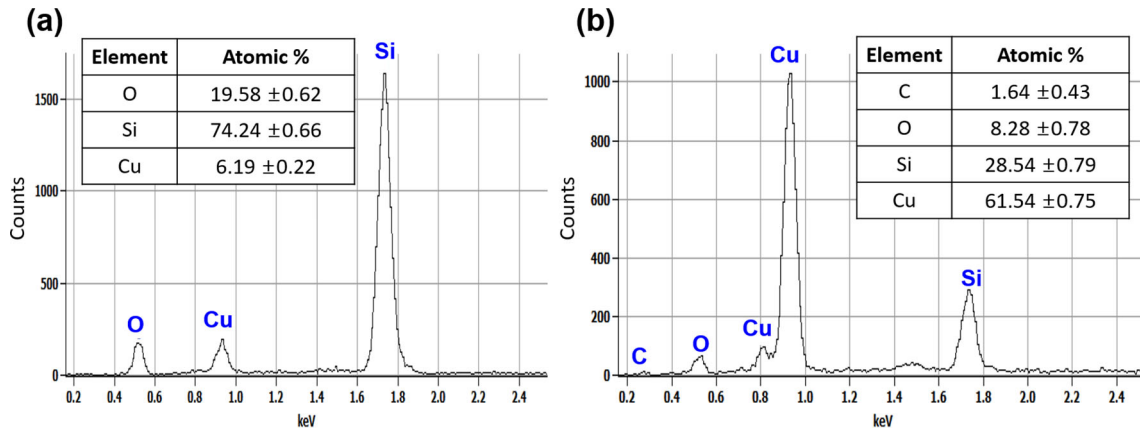


Fig. 5 Measured energy-dispersive X-ray spectra obtained at **a** the bottom SiNWs and **b** top Cu NW TPE; the tables in the graphs shows the detailed atomic compositions of the elements

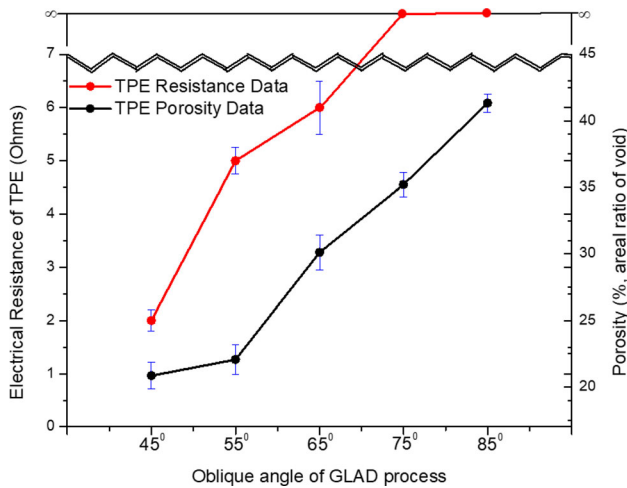


Fig. 6 Effect of the GLAD oblique angle on the electrical resistance and porosity of Cu NW TPEs with a thickness of 100 nm

between the fabricated vertical SiNW gas sensors due to the randomness of the GLAD process used in the fabrication of SiNWs and Cu TPE, different contact resistance of electrical wiring, different resistances of Cu TPE prepared by different fabrication conditions, and so on, the relative measured resistance (R_m/R_0) was selected as the sensor response, where R_m is the measured resistance between top and bottom electrodes at a specific relative humidity condition ($\sim 25\text{--}85\%$) and the R_0 is the resistance at the relative humidity of 25%. Figure 9 shows the effects of relative humidity on the sensor response (relative resistance, R_m/R_0). The relative resistance was decreased as increasing the humidity because the resistance of SiNWs were decreased when the water molecules absorbed on their surface. Figure 9 clearly shows the

linear co-relation between the relative humidity and R_m/R_0 as the value of R^2 is 0.99.

The sensing response or the sensitivity of the resistive type sensors can be determined as Eq. (1) [22–25].

$$\text{Sensitivity} = S = \frac{\Delta R}{R} = \frac{R_0 - R_{\min}}{R_0} \quad (1)$$

where R_0 refers to the resistance at relative humidity of 25% and R_{\min} represents the resistance of the sensors at relative humidity level of 85%. The sensitivity of the fabricated vertical SiNW sensor was defined as the change of relative resistances between at relative humidity values of 25% and 85%. Figure 10 illustrates the effects of (a) oblique angle and (b) thickness of the Cu TPE on humidity measurement sensitivity. The measured porosity values are also shown in Fig. 10. As can be clearly seen, the sensitivity increased with increasing oblique angle and decreasing thickness of the Cu TPE because it was mainly affected by the porosity of TPE [13]. Based on the sensitivity measurement results, an oblique angle of 65° and a deposition thickness of 100 nm was selected as the optimum Cu NW TPE GLAD fabrication conditions for the vertical SiNW sensor. Although the higher porosity could be obtained from the Cu TPE fabricated with higher oblique angle and thinner thickness, these fabrication conditions could not provide sufficient conductivity of Cu TPE which is essentially required for TPE of vertical SiNW gas sensor.

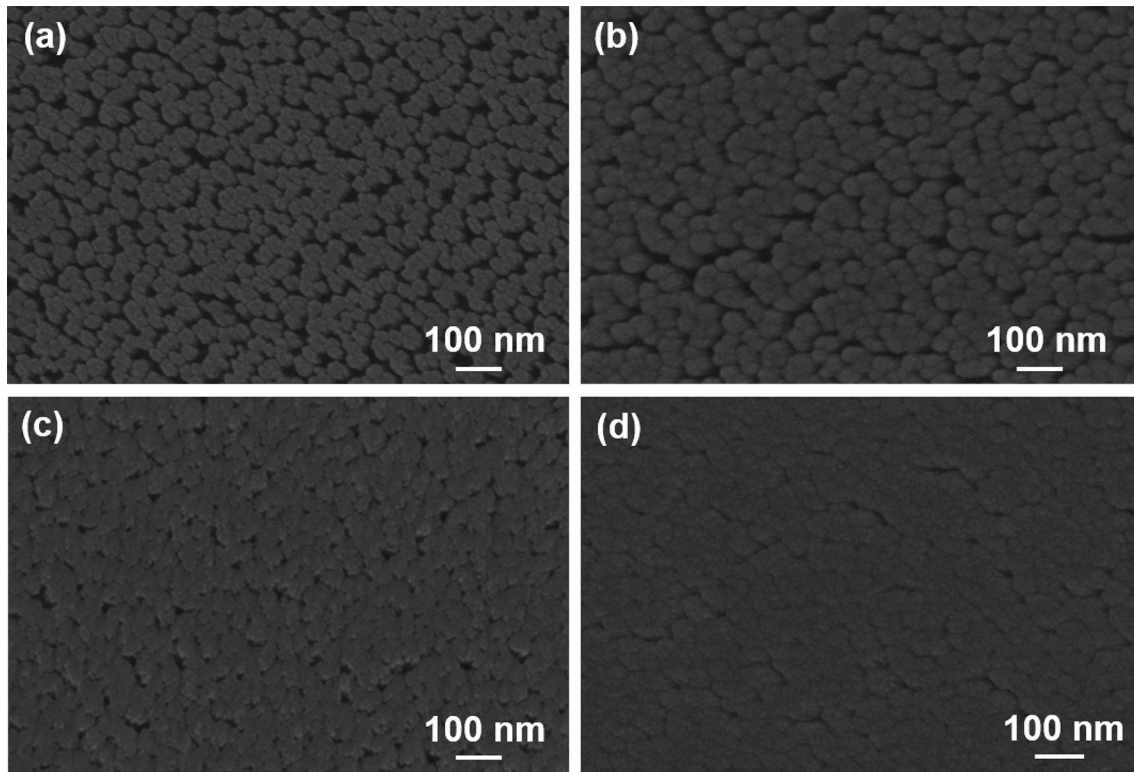


Fig. 7 Top-view SEM images of Cu NW TPEs with thicknesses of **a** 50, **b** 100, **c** 150, and **d** 200 nm. The GLAD oblique angle was fixed at 65°

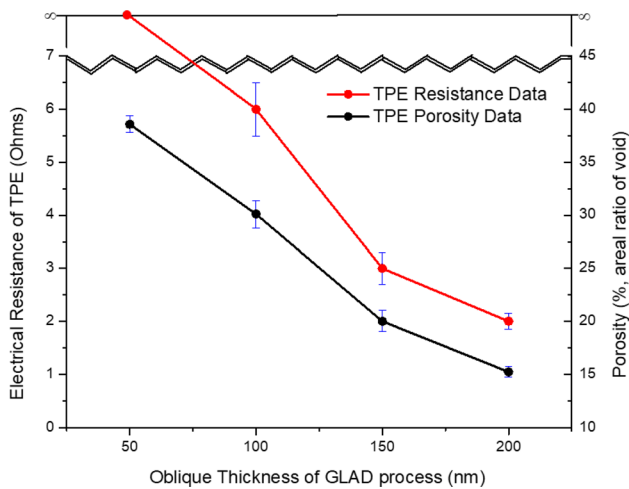


Fig. 8 Effects of Cu NW TPE thickness on the electrical resistance and porosity. The GLAD oblique angle was fixed at 65°

4 Conclusions

A cost-effective and large-area monolithic fabrication method for a vertical SiNW gas sensor using a simple two-step GLAD process is proposed and the performance of the fabricated sensor was evaluated using

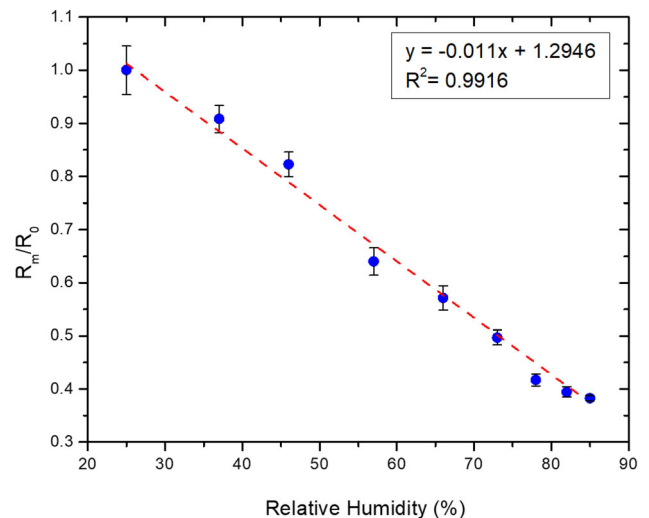


Fig. 9 Measured relative electrical resistance between the Si substrate and Cu NW TPE of the vertical SiNW gas sensor at various relative humidity conditions. The vertical SiNW gas sensor was fabricated by the proposed two-step GLAD process (1st step conditions: 85° oblique angle GLAD with 5 rpm substrate rotation for 1000 nm length SiNWs; second step condition: 65° oblique angle GLAD without substrate rotation for a 100 nm length Cu NW TPE)

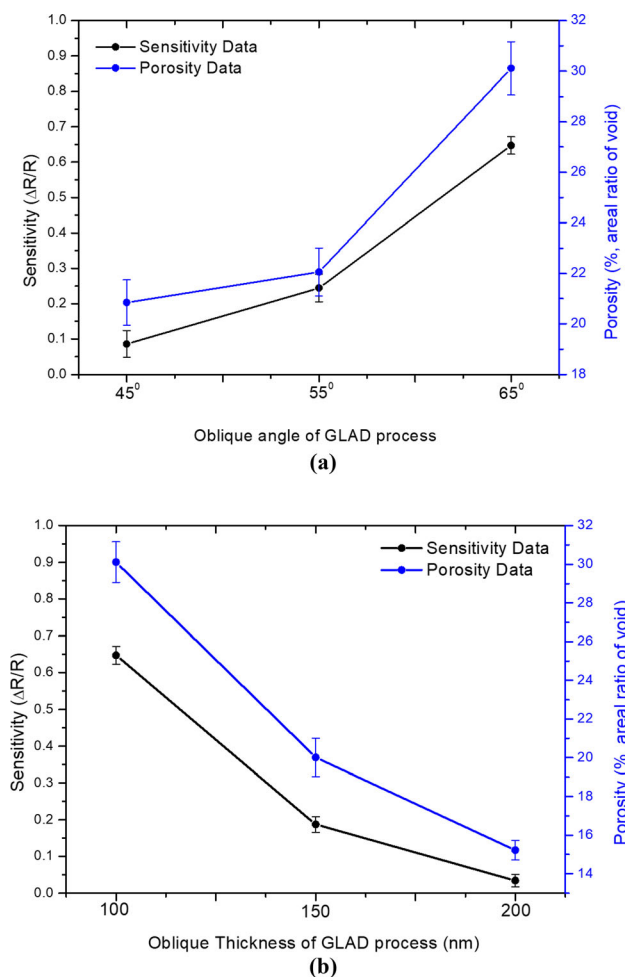


Fig. 10 Effects of **a** oblique angle at fixed thickness of 100 nm Cu NW and **b** a Cu NW thickness at fixed oblique angle of 65° on the sensitivity and porosity of a Cu NW TPE

relative humidity sensitivity measurements. The isolated vertical SiNWs with a diameter of ~ 90 nm and length of 1000 nm were successfully fabricated on a whole 4-inch Si substrate via GLAD at an oblique angle of 85° and with substrate rotation. The Cu TPE was also fabricated in the following GLAD without substrate rotation. As increasing the oblique angle in the Cu GLAD process, the porosity of Cu TPE was increased and the sensitivity was also increased because more gas analyte can pass through the pores on Cu TPE. However, with the oblique angle higher than 75°, the conductivity of the Cu TPE was too low to work as an electrode. As increasing the deposition thickness, the porosity of Cu TPE was decreased and the sensitivity was also decreased. However, the thickness of Cu TPE lower than 50 nm, we could not achieve sufficient conductivity due to fewer connections between Cu NWs. Based on the experimental comparisons, the Cu TPE GLAD process with an oblique angle of 65° and a

deposition thickness of 100 nm was selected as the optimum condition. The fabricated vertical SiNW gas sensor shows good linearity in the measurement of relative humidity. The analysis of the effects of morphological characteristics (various lengths, zigzag, spiral, etc.), crystalline structure, and doping concentration of SiNWs on the sensitivity and the application of the fabricated vertical SiNW gas sensor for real gas sensing applications are the subjects of ongoing research.

Authors' contributions

SK, XL, NA conceptualized and designed the experiments, NA, JK, JY, SL conducted the experiments, SK, XL, NA wrote and revised the manuscript. All authors read and approved the final manuscript.

Funding

This work was supported by Basic Science Research Program through the National Research Foundation of Korea (NRF) funded by the Ministry of Science, ICT & Future Planning (NRF-2020R1H1A2011487) and also supported by the Chung-Ang University Research Scholarship Grants in 2019.

Data availability

Data sharing is not applicable to this article as no datasets were generated or analyzed during the current study.

Compliance with ethical standards

Conflict of interest The authors declare that they have no competing interests.

References

1. M.C. McAlpine, H. Ahmad, D. Wang, J.R. Heath, Highly ordered nanowire arrays on plastic substrates for ultrasensitive flexible chemical sensors. *Nat. Mater.* **6**, 379–384 (2007). <https://doi.org/10.1038/nmat1891>
2. X. Zhou, J. Hu, C. Li, D. Ma, C. Lee, S. Lee, Silicon nanowires as chemical sensors. *Chem. Phys. Lett.* **369**, 220–224 (2003). [https://doi.org/10.1016/S0009-2614\(02\)02008-0](https://doi.org/10.1016/S0009-2614(02)02008-0)

3. Y. Engel, R. Elnathan, A. Pevzner, G. Davidi, E. Flaxer, F. Patolsky, Supersensitive detection of explosives by silicon nanowire arrays. *Angew. Chem.* **49**, 6830–6835 (2010). <https://doi.org/10.1002/anie.201000847>
4. J. Hahm, C.M. Lieber, Direct ultrasensitive electrical detection of DNA and DNA sequence variations using nanowire nanosensors. *Nano Lett.* **4**, 51–54 (2004). <https://doi.org/10.1021/nl034853b>
5. W.U. Wang, C. Chen, K. Lin, Y. Fang, C.M. Lieber, Label-free detection of small-molecule–protein interactions by using nanowire nanosensors. *Proc. Natl. Acad. Sci.* **102**, 3208–3212 (2005). <https://doi.org/10.1073/pnas.0406368102>
6. E. Stern, J.F. Klemic, D.A. Routenberg, P.N. Wyrembak, D.B. Turner-Evans, A.D. Hamilton, D.A. LaVan, T.M. Fahmy, M.A. Reed, Label-free immunodetection with CMOS-compatible semiconducting nanowires. *Nature.* **445**, 519–522 (2007). <https://doi.org/10.1038/nature05498>
7. D. Wang, H. Sun, A. Chen, S.-H. Jang, A.K.-Y. Jen, A. Szep, Chemiresistive response of silicon nanowires to trace vapor of nitro explosives. *Nanoscale.* **4**, 2628–2632 (2012). <https://doi.org/10.1039/C2NR30107E>
8. A. Cao, E. Sudhölter, L. de Smet, Silicon nanowire-based devices for gas-phase sensing. *Sensors.* **14**, 245–271 (2014). <https://doi.org/10.3390/s140100245>
9. Y. Cui, Q. Wei, H. Park, C.M. Lieber, Nanowire nanosensors for highly sensitive and selective detection of biological and chemical species. *Science.* **293**, 1289–1292 (2001). <https://doi.org/10.1126/science.1062711>
10. S. Zhao, Z. Li, G. Wang, J. Liao, S. Lv, Z. Zhu, Highly enhanced response of MoS₂/porous silicon nanowire heterojunctions to NO₂ at room temperature. *RSC adv.* **8**, 11070–11077 (2018). <https://doi.org/10.1039/C7RA13484C>
11. S. Choopun, N. Hongsih, E. Wongrat, *Metal-Oxide Nanowires for Gas Sensors. Nanowires-Recent Advances* (Intech open, London, 2012), pp. 3–24. <https://doi.org/10.5772/54385>
12. H. Li, J. Zhang, B. Tao, L. Wan, W. Gong, Investigation of capacitive humidity sensing behavior of silicon nanowires. *Physica E.* **41**, 600–604 (2009). <https://doi.org/10.1016/j.physe.2008.10.016>
13. H.J. In, C.R. Field, P.E. Pehrsson, Periodically porous top electrodes on vertical nanowire arrays for highly sensitive gas detection. *Nanotechnology.* **22**, 355501 (2011). <https://doi.org/10.1088/0957-4484/22/35/355501>
14. J. Ju, X. Huang, S.-M. Kim, J. Yeom, Fabrication of Highly Ordered Silicon Nanowires by Metal Assisted Chemical Etching Combined with a Nanoimprinting Process. *J. Nanosci. Nanotechnol.* **17**, 7771–7774 (2017)
15. K.-Q. Peng, X. Wang, S.-T. Lee, Gas sensing properties of single crystalline porous silicon nanowires. *Appl. Phys. Lett.* **95**, 243112 (2009). <https://doi.org/10.1063/1.3275794>
16. N. Abbas, X. Lu, M. Badshah, J. In, W. Heo, K. Park, M.-K. Lee, C. Kim, P. Kang, W.-J. Chang, Development of a Protein Microarray Chip with Enhanced Fluorescence for Identification of Semen and Vaginal Fluid. *Sensors.* **18**, 3874 (2018). <https://doi.org/10.3390/s18113874>
17. M.M. Hawkeye, M.J. Brett, Glancing angle deposition: Fabrication, properties, and applications of micro- and nanostructured thin films. *J. Vac. Sci. Technol. A.* **25**, 1317–1335 (2007). <https://doi.org/10.1116/1.2764082>
18. H. Jang, G. Shin, H. Jang, J. Ju, J. Lim, S. Kim, Design and Fabrication of Wire Grid Polarizer by Nanoimprinting and Glancing Angle Deposition Processes. *Mater. Trans.* **58**(3), 494–498 (2017). <https://doi.org/10.2320/matertrans.M2016219>
19. M.A. Badshah, J. Ju, X. Lu, N. Abbas, S. Kim, Enhancing the sensitivity of DNA microarrays by metal-enhanced fluorescence using vertical nanorod structures. *Sensor. Actuat. B-Chem.* **274**, 451–457 (2018). <https://doi.org/10.1016/j.snb.2018.07.163>
20. D.P. Singh, S. Kumar, J. Singh, Morphology dependent surface enhanced fluorescence study on silver nanorod arrays fabricated by glancing angle deposition. *RSC Adv.* **5**, 31341–31346 (2015). <https://doi.org/10.1039/C5RA03225C>
21. X. Lu, S. Kim, S.J. Seo, Fabrication of a large-area superhydrophobic SiO₂ nanorod structured surface using glancing angle deposition. *J. Nanomater.* (2017). <https://doi.org/10.1155/2017/8305439>
22. X. Chen, J. Zhang, Z. Wang, Q. Yan, S. Hui, Humidity sensing behavior of silicon nanowires with hexamethyldisilazane modification. *Sensor. Actuat. B-Chem.* **156**, 631–636 (2011). <https://doi.org/10.1016/j.snb.2011.02.009>
23. A. Tripathy, S. Pramanik, J. Cho, J. Santhosh, N.A. Abu Osman, Role of morphological structure, doping, and coating of different materials in the sensing characteristics of humidity sensors. *Sensors.* **14**, 16343–16422 (2014). <https://doi.org/10.3390/s140916343>
24. J. Chu, X. Peng, P. Feng, Y. Sheng, J. Zhang, Study of humidity sensors based on nanostructured carbon films produced by physical vapor deposition. *Sensor. Actuat. B-Chem.* **178**, 508–513 (2013). <https://doi.org/10.1016/j.snb.2012.12.104>
25. Y. Feng, S. Gong, E. Du, K. Yu, J. Ren, Z. Wang, Z. Zhu, Ta₂S₂ nanosheet-based ultrafast response and flexible humidity sensor for multifunctional applications. *J. Mater. Chem. C.* **7**, 9284–9292 (2019). <https://doi.org/10.1039/C9TC02785H>

Publisher's note Springer Nature remains neutral with regard to jurisdictional claims in published maps and institutional affiliations.